

LDPM: Towards undersampled MRI reconstruction with MR-VAE and Latent Diffusion Prior

Xingjian TANG[†]
Shenzhen Technology University
Shenzhen University
2310417007@stumail.sztu.edu.cn

Jingwei GUAN^{†*}
Shenzhen Technology University
guanjingwei@sztu.edu.cn

Linge LI
Huawei
lilinge@huawei.com

Youmei ZHANG
Qilu University of Technology
zhangyoumei@qlu.edu.cn

Mengye LYU
Shenzhen Technology University
lvmengye@sztu.edu.cn

Li YAN^{*}
Shenzhen Technology University
yanli@sztu.edu.cn

Abstract—Diffusion model, as a powerful generative model, has found a wide range of applications including MRI reconstruction. However, most existing diffusion model-based MRI reconstruction methods operate directly in pixel space, which makes their optimization and inference computationally expensive. Latent diffusion models were introduced to address this problem in natural image processing, but directly applying them to MRI reconstruction still faces many challenges, including the lack of control over the generated results, the adaptability of Variational AutoEncoder (VAE) to MRI, and the exploration of applicable data consistency in latent space. To address these challenges, a Latent Diffusion Prior based undersampled MRI reconstruction (LDPM) method is proposed. A sketcher module is utilized to provide appropriate control and balance the quality and fidelity of the reconstructed MR images. A VAE adapted for MRI tasks (MR-VAE) is explored, which can serve as the backbone for future MR-related tasks. Furthermore, a variation of the DDIM sampler, called the Dual-Stage Sampler, is proposed to achieve high-fidelity reconstruction in the latent space. The proposed method achieves competitive results on fastMRI datasets, and the effectiveness of each module is demonstrated in ablation experiments.

Index Terms—Latent Diffusion Prior, MRI reconstruction, Variational Autoencoder (VAE)

I. INTRODUCTION

Magnetic Resonance Imaging (MRI) is a non-invasive medical imaging technique frequently used for disease diagnosis and treatment. However, the long scan time limits its broader application. To this end, k-space undersampling technique is employed to accelerate MRI acquisition. High acceleration factors (AF) can introduce aliasing artifacts, which need to be removed through reconstruction to achieve diagnostic-quality MRI [7]. Methods like parallel imaging [35]–[37] and compressed sensing [31]–[34] were proposed to enhance MRI reconstruction, but they still suffer from limitations like residual artifacts and blurring [30].

In recent years, deep learning methods have been developed into the mainstream techniques for addressing undersampled MRI reconstruction problems [3], [6], [7], [23]–[25], especially those based on diffusion models (DMs, [13], [14], [20]).

The authors with [†] contributed to the work equally and should be regarded as co-first authors. Corresponding authors are marked with *.

Chung et al. [1] proposed an SDE model that shows great reconstruction outcomes in various modalities and diverse body parts. Cao et al. [4] trained a DM with only high frequency MR k-space to preserve the consistency of the acquired low frequency information. Güngör et al. [8] utilized the sensitivity maps to enhance inference performance with large step diffusion. Peng et al. [12] proposed a model that visualizes multiple potential reconstructions and employing a novel method to estimate the most likely one. DM-based methods have demonstrated exceptional performance in reconstructing MR images [5], [39], [40]. Nevertheless, most of these methods operate directly in pixel domains (e.g., image domain and k-space), where optimization and inference are computationally demanding, making them more difficult to be applied in medical settings. Therefore, a more lightweight method is needed to enhance the accessibility of DM and reduce its significant resource consumption.

Utilizing latent diffusion models (LDMs) [15], [21] is one of the solutions for light-weighted natural image reconstruction [16], [22], [27]–[29]. However, direct application of LDMs to the task of MRI reconstructions still faces several challenges. **Firstly**, although the vanilla LDM framework exhibits superior performance in image generation, it may focus more on image quality rather than fidelity [2], [16] and requires appropriate control. **Secondly**, pre-trained variational autoencoders (VAEs) [18] are utilized in LDMs to map pixel-domain images into the latent space. As a lossy compression model [26], current VAEs pre-trained on natural images may lead to information misinterpretation on MRI images [22]. **Finally**, the widely used operation to ensure the fidelity of MRI reconstruction, data consistency (DC), needs to be modified to adapt to the LDM-based framework and address possible artifacts [9]. In order to fully exploit the advantages of LDM and solve these problems as much as possible, an undersampled MRI reconstruction method LDPM is proposed. To conclude, the main contributions of this work are:

- An MR-VAE and Latent Diffusion Prior based undersampled MRI reconstruction model (LDPM) is proposed. The latent diffusion model enables diffusion model training and inference on limited computational resources. More-

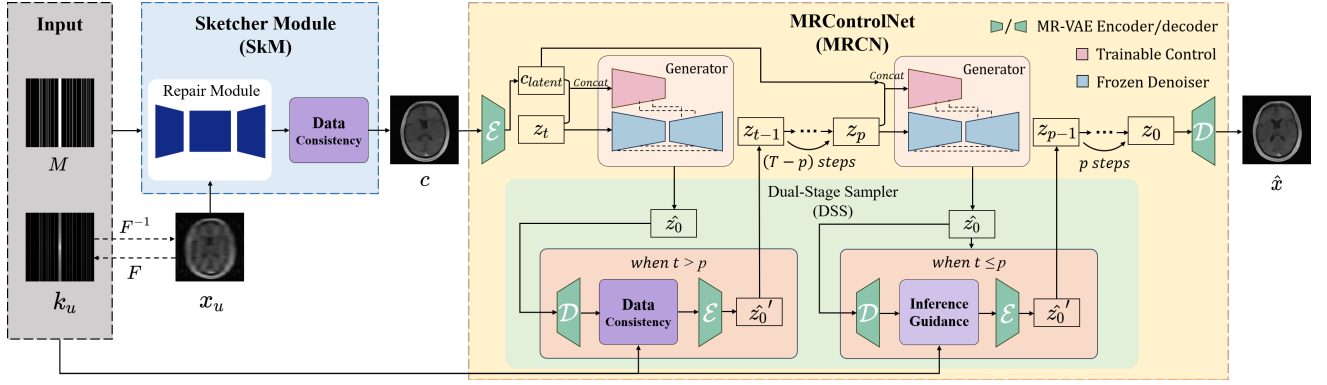


Fig. 1. Pipeline of the proposed LDPM method. 1) The Sketcher Module removes the artifacts and generates sketch image c as the condition. 2) MRControlNet generates fully-sampled MRI prediction \hat{x} with MR-VAE and Dual-Stage sampler for higher fidelity.

over, a sketcher module is utilized to produce conditional controls to ensure accurate detail generation in large scale undersample problems, which helps balance quality and fidelity of reconstructed MR images.

- A MR-VAE is proposed and can be utilized as the backbone for the future MR-related tasks to transfer image to the latent domain. The MR-VAE is proved effective to minimize the loss in MRI images reconstruction and further improve the detail reconstruction results for undersampled MRI reconstruction tasks.
- A variant of the DDIM sampler [10], named the Dual-Stage Sampler, is proposed to enable high-fidelity reconstruction to the LDM-based framework and address possible artifacts.

II. METHOD

The proposed MRI reconstruction method LDPM (Φ) aims at reconstructing the fully-sampled image \hat{x} from the undersampled k-space k_u and its undersampling mask M as (1).

$$\hat{x} = \Phi(k_u, M) \quad (1)$$

Φ consists of two main modules, namely the sketcher module and MRControlNet, as shown in 1. First, a transformer-based sketcher module (SkM) is used to generate artifact-free MRI sketches. Then a ControlNet-based [11] model MRControlNet (MRCN) is designed to control precise reconstruction details according to the conditions generated in the SkM.

A. Sketcher Module (SkM)

To ensure reliable conditional information for ControlNet-based pipeline functions, we introduce the sketcher module (SkM) ϕ_1 to generate an appropriate conditional image c from M and an undersampled image $x_u = F^{-1}(k_u)$, where F^{-1} represents the inverse Fourier transform operator.

$$c = \phi_1(x_u, M). \quad (2)$$

In ϕ_1 , a SwinIR [17]-based repair model R is first utilized, which can effectively erase aliases in x_u and conduct the LDM focus more on generating realistic details [2]. Following the repair module, the data consistency (DC) operation is

employed to improve data fidelity of the condition c . The DC operation can be expressed as:

$$c = DC[R(x_u), k_u, M] = F^{-1}\{F[R(x_u)] \cdot (I - M) + k_u \cdot M\}, \quad (3)$$

where I denotes the all-ones matrix, F denotes the forward Fourier transform operator.

B. MRControlNet (MRCN)

The MRControlNet (MRCN) ϕ_2 is intended to reconstruct the full-sampled image \hat{x} under the control of the condition image c , as illustrated in Fig. 1. Three key parts are involved in MRCN, including 1) MR-VAE, 2) Generator and 3) Dual-Stage Sampler (DSS).

$$\hat{x} = \phi_2(k_u, M, c). \quad (4)$$

1) *MR-VAE*: VAE is an important module to map images into the latent space. Although many natural image restoration methods [2], [16] tend to keep pre-trained VAE weights in stable diffusion (SD) [15], such VAEs have not been exposed to MRI images during training and therefore cannot be directly generalized to the MRI domain for accurate MRI detail restoration. To address this issue, we propose MR-VAE, a VAE that can be used for various MR-related tasks. MR-VAE is finetuned on SD pre-train [15] to leverage its rich generative prior. The encoder and decoder are utilized in the reconstruction process and optimized with three terms of loss functions. The pixel loss and VGG loss are utilized to reduce the pixel-wise difference; the KL-divergence loss is also introduced to ensure that the generated latent code meets the prior requirements of the diffusion model. The total loss can be expressed as:

$$L_{vae} = \mu \cdot \|\hat{x}_{vae} - x\|_1 + \nu \cdot \|VGG(\hat{x}_{vae}) - VGG(x)\|_1 + \omega \cdot \text{KL}(N(u, \sigma^2) \| N(0, 1)), \quad (5)$$

where \hat{x}_{vae} denotes the reconstruction result of MR-VAE, VGG denotes VGG network [19], u and σ denote the mean and variance of the reconstruction distribution, respectively. As shown in Fig. 3, MR-VAE produces more realistic reconstructions on MRI data than the VAE in SD.

2) *Generator*: In the generator, a trainable control and a frozen denoiser are utilized. The trainable copy of the pre-trained U-Net down-sampler and middle block from SD [15] are conducted, which preserves generative diffusion prior that trained on a large-scale natural image dataset. The condition latent $c_{latent} = \mathcal{E}(c)$ and noisy latent z_t are concatenated together as the input of the frozen denoiser. z_t at time step t can be denoted as:

$$z_t = \sqrt{\alpha_t}z + \sqrt{1 - \alpha_t}\epsilon, \quad (6)$$

where z is a latent code encoded from image x ($z = \mathcal{E}(x)$), α_t is from a decreasing sequence where $\alpha_{1:T} \in (0, 1]^T$, and the noise $\epsilon \sim \mathcal{N}(0, \mathbf{I})$. The channel number is increased by the concatenate operation. thus We follow the setup of IRControlNet [2], appending some extra parameters and then initializing them to zero to avoid noisy gradients in early training steps. The training loss can be denoted as:

$$L_{MRCN} = \mathbb{E}_{z_t, p, t, \epsilon, c_{latent}} \left[\|\epsilon - \epsilon_\theta(z_t, p, t, c_{latent})\|_2^2 \right], \quad (7)$$

where p is the condition input (i.e., text prompt) and ϵ_θ is the learned noise-predicting network.

3) *Dual-Stage Sampler (DSS)*: To achieve high-fidelity latent sampling while avoiding the introduction of additional artifacts, a deterministic variant of the DDIM sampler named Dual-Stage Sampler (DSS) [10] is proposed. A two-stage operation based on the time step t is utilized in DSS. At each time step t , clean latent \hat{z}_0 is predicted through (8):

$$\epsilon_t = \epsilon_\theta(z_t, p, t, c_{latent}), \hat{z}_0 = \sqrt{\alpha_{t-1}} \left(\frac{z_t - \sqrt{1 - \alpha_t} \epsilon_t}{\sqrt{\alpha_t}} \right) \quad (8)$$

The division of stages is determined by the constant time p , which is set to 200. When $t > p$, data consistency (DC) is utilized. The DC operation (9) substitutes the corresponding k-space area in the clean image prediction $\hat{x}_0 = \mathcal{D}(\hat{z}_0)$ with estimated data k_u , which improves data fidelity. However, it may introduce some unwanted artifacts when processing the magnitude images [9]. Thus, DC is only employed in the early sampling steps ($t > p$) where the level of noise is higher.

$$\hat{z}_0' = \mathcal{E}[DC(\hat{x}_0, k_u, M)] \quad (9)$$

When $t \leq p$, k-space inference guidance that modified from restoration guidance [2] is employed to generate artifact-free and more realistic images. In this stage, we first calculate δ , the L2 loss between the masked k-space prediction $F(\hat{x}_0)$ and the estimated k-space k_u as shown in (10), then the generation is guided by δ through (11).

$$\delta = \mathcal{E}\{\|F(\hat{x}_0) - k_u\|_2^2\}, \quad (10)$$

$$\hat{z}_0' = \hat{z}_0 - g \nabla_{\hat{z}_0} \delta, \quad (11)$$

where g is the guidance scale and is set into 0.1. z_{t-1} is sampled from z_t via the standard deviation of Gaussian noise at time t (σ_t):

$$z_{t-1} = \hat{z}_0' + \sqrt{1 - \alpha_{t-1} - \sigma_t^2} \cdot \epsilon_t, \quad (12)$$

TABLE I
QUANTITATIVE EVALUATION ON THE FASTMRI DATASET [7]

Method	PSNR \uparrow	SSIM \uparrow	FID \downarrow
Zero-Filled	23.9467	0.6817	265.0842
U-Net [7]	26.7036	0.6212	52.6383
E2E-VarNet [6]	30.0438	0.6659	34.5586
SwinMR [3]	30.0008	0.8407	60.6761
Score-MRI [1]	29.6848	0.7978	15.7723
LDPM (Ours)	30.0764	0.8135	28.8984

Bold and **Bold italic** indicate the best and second best score.

III. EXPERIMENTAL RESULTS

A. Dataset and Implementation Details

1) *Dataset*: All the experiments were conducted on the fastMRI brain dataset [7], including multi-coil brain scans of FLAIR-, T1- and T2-weighted MR images. For each subject, the last 3 slices were discarded due to poor image quality. In training, images from 1793 subjects were utilized (a total of 23275 slices, with 2500 slices used for validation). For testing, 72 subjects were involved (a total of 934 slices). All multi-coil MR images were processed into coil-combined magnitude images using the root-sum-of-squares (RSS) [7].

2) *Implementation Details*: First, the sketcher module (SkM) was trained with a learning rate (lr) of $1e - 4$, a batch size (bs) of 8, and used random cropping (of size 96) and flipping for dataset augmentation. Then, the MR-VAE is fine-tuned based on the pre-trained stable diffusion 2-1-base [15] with $lr = 10e - 5$, $bs = 8$, $\mu = 1$, $\nu = 0.01$, and $\omega = 1e - 8$. Next, MRCN was trained based on MR-VAE with the patchsize of 320×320 , $lr = 10e - 4$, $bs = 16$, and $T = 1000$, where MR-VAE was fixed during training. Prompt condition was set to empty. SkM was trained for 30 epochs, MR-VAE for 50 epochs and the generator for 50 epochs.

B. Quantitative and Visual Evaluation

The proposed LDPM method is intuitively and quantitatively evaluated and compared with several classic and state-of-the-art methods, including zero-filled reconstruction, U-Net [7], E2E-VarNet [6], SwinMR (nPI version) [3], and score-MRI [1]. The official pre-trained models of U-Net [7] and E2E-VarNet [6] are used. Both SwinMR [3] and Score-MRI [1] were trained according to their official instructions, with $N = 2000$ in ScoreMRI following the official settings. The quantitative evaluation results are shown in Table I with an acceleration factor (AF) of 8. The proposed method outperforms all other algorithms, achieving the highest PSNR and also ranking as the second-best in SSIM [38] and FID [41]. This demonstrates its competitive reconstruction ability.

Two groups of test result examples of state-of-the-art methods are shown in Fig. 2. The reconstruction results generated by U-Net [7] lose some fine details and sometimes suffer from color distortion, as shown in **A3**. E2E-VarNet [6] exhibits smoothing and residual artifacts, e.g., the reconstruction in **b4** has an obvious additional texture that is not found in

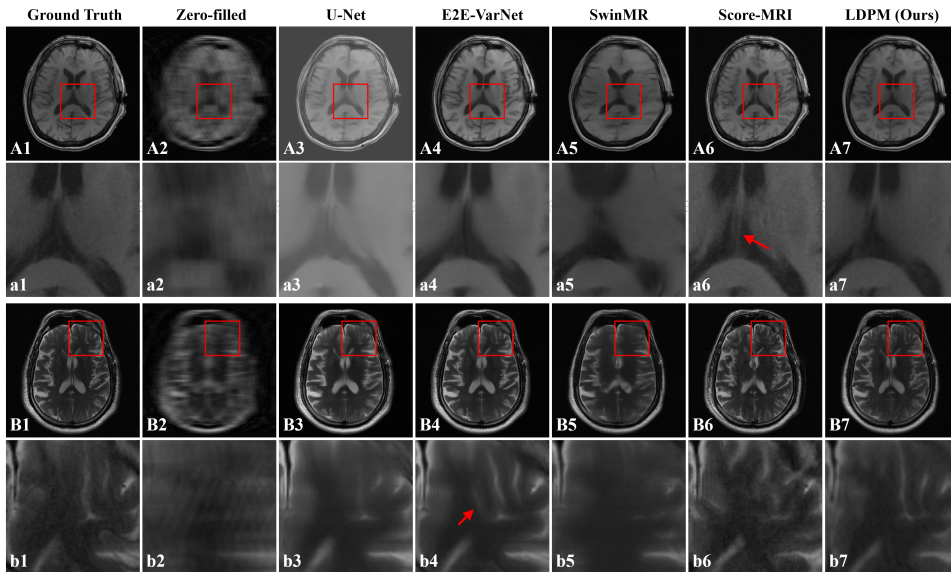


Fig. 2. Examples of visual results of MRI reconstruction methods under $8\times$ acceleration. **A1-A7&B1-B7**: full images; **a1-a7&b1-b7**: zoomed-in patches.

TABLE II
QUANTITATIVE EVALUATION OF ABLATION EXPERIMENTS

Models	PSNR	SSIM
LDPM (w/o SkM)	25.7746	0.7259
LDPM (w/o MR-VAE)	26.2837	0.7166
LDPM (w/o DSS)	29.7573	0.7948
LDPM (Ours)	30.0764	0.8135

the ground-truth image **b1**. SwinMR [3] suffers from severe detail loss, resulting in reconstructions lacking texture in both examples. Score-MRI [1] tends to generate images with unrealistic details stochastically, as shown in both examples **a6**, **b6**, which may cause interference in medical diagnosis. The proposed LDPM method achieves the best artifact-free reconstruction results with realistic details, demonstrating the powerful generalization ability of the latent fusion prior.

C. Effectiveness of SkM, MR-VAE and DSS

The effectiveness of each component, including SkM, MR-VAE, and DSS, was examined through a series of ablation studies. Results are shown in Table II. It can be seen that the removal of each component will lead to losses in PSNR and SSIM [38], proving that each component is effective.

In particular, MR-VAE is carefully compared with the VAE that is widely used as a pre-trained VAE on natural images (VAE in SD [15]), as shown in Fig. 2. Quantitative evaluation with PSNR and SSIM [38] were conducted on the 934 testing images. The higher scores of SSIM [38] and PSNR prove that MR-VAE is more suitable for MRI reconstruction tasks than VAE in SD [15]. A closer look at the zoomed-in detail patches indicated by arrows reveals that MR-VAE can provide

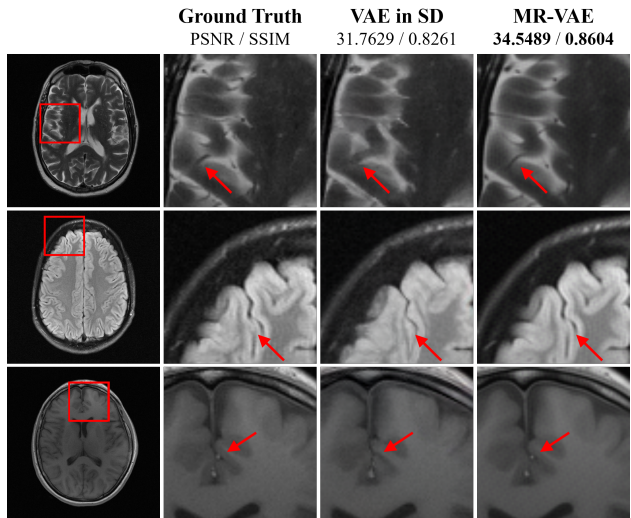


Fig. 3. Visual and quantitative comparison of MR-VAE reconstruction results with that of VAE in SD [15]. Objective metrics include PSNR and SSIM [38]. Subjective results include the full images and zoomed-in patches.

more realistic details, while VAE in SD [15] often produces incorrect structures, leading to misinterpretation.

IV. CONCLUSION

In this work, a latent diffusion prior based MRI reconstruction method LDPM is proposed. An MRI prior-enhanced MR-VAE and a latent space-appropriate Dual-Stage Sampler are proposed to reduce the latent space transformation loss and improve the reconstruction fidelity, respectively. The LDPM method outperforms the state-of-the-art methods and demonstrates the potential of applying latent diffusion priors in future MRI reconstruction studies.

REFERENCES

- [1] H. Chung and J. C. Ye, "Score-based diffusion models for accelerated mri," *Med. Image Anal.*, vol. 80, p. 102479, 2022.
- [2] X. Lin, J. He, Z. Chen, Z. Lyu, B. Dai, F. Yu, W. Ouyang, Y. Qiao, and C. Dong, "Diffbir: Towards blind image restoration with generative diffusion prior," *arXiv preprint arXiv:2308.15070*, 2023.
- [3] J. Huang, Y. Fang, Y. Wu, H. Wu, Z. Gao, Y. Li, J. Del Ser, J. Xia, and G. Yang, "Swin transformer for fast mri," *Neurocomputing*, vol. 493, pp. 281–304, 2022.
- [4] C. Cao, Z.-X. Cui, Y. Wang, S. Liu, T. Chen, H. Zheng, D. Liang, and Y. Zhu, "High-frequency space diffusion model for accelerated mri," *IEEE Trans. Med. Imaging*, 2024.
- [5] C. Zhang, Y. Chen, Z. Fan, Y. Huang, W. Weng, R. Ge, D. Zeng, and C. Wang, "Tc-diffrecon: Texture coordination mri reconstruction method based on diffusion model and modified mf-unet method," *arXiv preprint arXiv:2402.11274*, 2024.
- [6] A. Sriram, J. Zbontar, T. Murrell, A. Defazio, C. L. Zitnick, N. Yakubova, F. Knoll, and P. Johnson, "End-to-end variational networks for accelerated mri reconstruction," *Lect. Notes Comput. Sci.*, pp. 64–73, 2020.
- [7] J. Zbontar, F. Knoll, A. Sriram, T. Murrell, Z. Huang, M. J. Muckley, A. Defazio, R. Stern, P. Johnson, M. Bruno *et al.*, "fastmri: An open dataset and benchmarks for accelerated mri," *arXiv preprint arXiv:1811.08839*, 2018.
- [8] A. Güngör, S. U. Dar, Ş. Öztürk, Y. Korkmaz, H. A. Bedel, G. Elmas, M. Ozbey, and T. Çukur, "Adaptive diffusion priors for accelerated mri reconstruction," *Med. Image Anal.*, vol. 88, p. 102872, 2023.
- [9] Z. Gao and S. K. Zhou, "U2mrpd: Unsupervised undersampled mri reconstruction by prompting a large latent diffusion model," *arXiv preprint arXiv:2402.10609*, 2024.
- [10] J. Song, C. Meng, and S. Ermon, "Denoising diffusion implicit models," *Int. Conf. Learn. Represent., ICLR*, 2020.
- [11] L. Zhang, A. Rao, and M. Agrawala, "Adding conditional control to text-to-image diffusion models," *Proc. IEEE Int. Conf. Comput. Vision*, pp. 3836–3847, 2023.
- [12] C. Peng, P. Guo, S. K. Zhou, V. M. Patel, and R. Chellappa, "Towards performant and reliable undersampled mr reconstruction via diffusion model sampling," *Int. Conf. Learn. Represent., ICLR*, pp. 623–633, 2022.
- [13] J. Ho, A. Jain, and P. Abbeel, "Denoising diffusion probabilistic models," *Adv. neural inf. proces. syst.*, vol. 33, pp. 6840–6851, 2020.
- [14] Y. Song and S. Ermon, "Generative modeling by estimating gradients of the data distribution," *Adv. neural inf. proces. syst.*, vol. 32, 2019.
- [15] R. Rombach, A. Blattmann, D. Lorenz, P. Esser, and B. Ommer, "High-resolution image synthesis with latent diffusion models," *Proc. IEEE Comput. Soc. Conf. Comput. Vision Pattern Recognit.*, pp. 10 684–10 695, 2022.
- [16] J. Wang, Z. Yue, S. Zhou, K. C. Chan, and C. C. Loy, "Exploiting diffusion prior for real-world image super-resolution," *Int. J. Comput. Vision*, pp. 1–21, 2024.
- [17] J. Liang, J. Cao, G. Sun, K. Zhang, L. Van Gool, and R. Timofte, "Swinir: Image restoration using swin transformer," *Proc. IEEE. Int. Conf. Comput. Vision*, pp. 1833–1844, 2021.
- [18] D. P. Kingma, "Auto-encoding variational bayes," *arXiv preprint arXiv:1312.6114*, 2013.
- [19] K. Simonyan and A. Zisserman, "Very deep convolutional networks for large-scale image recognition," *arXiv preprint arXiv:1409.1556*, 2014.
- [20] Y. Song, J. Sohl-Dickstein, D. P. Kingma, A. Kumar, S. Ermon, and B. Poole, "Score-based generative modeling through stochastic differential equations," *Int. Conf. Learn. Represent., ICLR*, 2020.
- [21] A. Vahdat, K. Kreis, and J. Kautz, "Score-based generative modeling in latent space," *Adv. neural inf. proces. syst.*, vol. 34, pp. 11 287–11 302, 2021.
- [22] F. Yu, J. Gu, Z. Li, J. Hu, X. Kong, X. Wang, J. He, Y. Qiao, and C. Dong, "Scaling up to excellence: Practicing model scaling for photo-realistic image restoration in the wild," *Proc. IEEE Comput. Soc. Conf. Comput. Vision Pattern Recognit.*, pp. 25 669–25 680, 2024.
- [23] G. Yang, S. Yu, H. Dong, G. Slabaugh, P. L. Dragotti, X. Ye, F. Liu, S. Arridge, J. Keegan, Y. Guo *et al.*, "Dagan: deep de-aliasing generative adversarial networks for fast compressed sensing mri reconstruction," *IEEE Trans. Med. Imaging*, pp. 1310–1321, 2017.
- [24] P. Guo, Y. Mei, J. Zhou, S. Jiang, and V. M. Patel, "Reconformer: Accelerated mri reconstruction using recurrent transformer," *IEEE Trans. Med. Imaging*, 2023.
- [25] B. Zhou and S. K. Zhou, "Dudornet: learning a dual-domain recurrent network for fast mri reconstruction with deep t1 prior," *Proc. IEEE Comput. Soc. Conf. Comput. Vision Pattern Recognit.*, pp. 4273–4282, 2020.
- [26] L. Theis, W. Shi, A. Cunningham, and F. Huszár, "Lossy image compression with compressive autoencoders," *Int. Conf. Learn. Represent., ICLR*, 2017.
- [27] Z. Luo, F. K. Gustafsson, Z. Zhao, J. Sjölund, and T. B. Schön, "Refusion: Enabling large-size realistic image restoration with latent-space diffusion models," *Proc. IEEE Comput. Soc. Conf. Comput. Vision Pattern Recognit.*, pp. 1680–1691, 2023.
- [28] D. Zheng, X.-M. Wu, S. Yang, J. Zhang, J.-F. Hu, and W.-S. Zheng, "Selective hourglass mapping for universal image restoration based on diffusion model," *Proc. IEEE Comput. Soc. Conf. Comput. Vision Pattern Recognit.*, pp. 25 445–25 455, 2024.
- [29] T. Varanka, T. Toivonen, S. Tripathy, G. Zhao, and E. Acar, "Pfstorer: Personalized face restoration and super-resolution," *Proc. IEEE Comput. Soc. Conf. Comput. Vision Pattern Recognit.*, pp. 2372–2381, 2024.
- [30] K. Sun, Q. Wang, and D. Shen, "Joint cross-attention network with deep modality prior for fast mri reconstruction," *IEEE Trans. Med. Imaging*, 2023.
- [31] D. L. Donoho, "Compressed sensing," *IEEE Trans. Inf. Theory*, vol. 52, no. 4, pp. 1289–1306, 2006.
- [32] S. G. Lingala, Y. Hu, E. DiBella, and M. Jacob, "Accelerated dynamic mri exploiting sparsity and low-rank structure: kt slr," *IEEE Trans. Med. Imaging*, vol. 30, no. 5, pp. 1042–1054, 2011.
- [33] B. Zhao, J. P. Haldar, A. G. Christodoulou, and Z.-P. Liang, "Image reconstruction from highly undersampled (k, t)-space data with joint partial separability and sparsity constraints," *IEEE Trans. Med. Imaging*, vol. 31, no. 9, pp. 1809–1820, 2012.
- [34] A. Majumdar, "Improving synthesis and analysis prior blind compressed sensing with low-rank constraints for dynamic mri reconstruction," *Magn. Reson. Imaging*, vol. 33, no. 1, pp. 174–179, 2015.
- [35] K. P. Pruessmann, M. Weiger, M. B. Scheidegger, and P. Boesiger, "Sense: sensitivity encoding for fast mri," *Magn. Reson. Med.*, vol. 42, no. 5, pp. 952–962, 1999.
- [36] M. A. Griswold, P. M. Jakob, R. M. Heidemann, M. Nittka, V. Jellus, J. Wang, B. Kiefer, and A. Haase, "Generalized autocalibrating partially parallel acquisitions (grappa)," *Magn. Reson. Med.*, vol. 47, no. 6, pp. 1202–1210, 2002.
- [37] M. Lustig and J. M. Pauly, "Spirit: iterative self-consistent parallel imaging reconstruction from arbitrary k-space," *Magn. Reson. Med.*, vol. 64, no. 2, pp. 457–471, 2010.
- [38] Z. Wang, A. C. Bovik, H. R. Sheikh, and E. P. Simoncelli, "Image quality assessment: from error visibility to structural similarity," *IEEE Trans. Image Process.*, vol. 13, no. 4, pp. 600–612, 2004.
- [39] S. Huang, G. Luo, X. Wang, Z. Chen, Y. Wang, H. Yang, P.-A. Heng, L. Zhang, and M. Lyu, "Noise level adaptive diffusion model for robust reconstruction of accelerated mri," *arXiv preprint arXiv:2403.05245*, 2024.
- [40] S. Huang, G. Luo, Y. Wang, K. Yang, L. Zhang, J. Liu, H. Guo, M. Wang, and M. Lyu, "Robust simultaneous multislice mri reconstruction using deep generative priors," *arXiv preprint arXiv:2407.21600*, 2024.
- [41] M. Heusel, H. Ramsauer, T. Unterthiner, B. Nessler, and S. Hochreiter, "Gans trained by a two time-scale update rule converge to a local nash equilibrium," *Adv. neural inf. proces. syst.*, vol. 30, 2017.